MJFAS MALAYSIAN JOURNAL OF FUNDAMENTAL AND APPLIED SCIENCES
PRINT ISSN: 2289-5981 | ONLINE ISSN: 2289-599X

RESEARCH ARTICLE

Free convection boundary layer flow over a horizontal circular cylinder in Al_2O_3-Ag/water hybrid nanofluid with viscous dissipation

Muhammad Khairul Anuar Mohamed [a,*], Mohd Zuki Salleh [a], Fadhilah Che Jamil [b], Ong Huei Ruey [b]

[a] Centre for Mathematical Sciences, Universiti Malaysia Pahang, 26300 UMP Kuantan, Pahang, MALAYSIA.
[b] Faculty of Engineering, DRB-HICOM University of Automotive Malaysia, Peramu Jaya Industrial Area, 26607 Pekan, Pahang, MALAYSIA.

* Corresponding author: mkhairulanuar@ump.edu.my

Article history
Received 3 June 2020
Revised 7 September 2020
Accepted 22 September 20220

Abstract

In this paper, the mathematical model of free convection boundary layer flow of horizontal circular cylinder immersed in *Ag/Water* nanofluid and Al_2O_3-*Ag/Water* hybrid nanofluid are considered. The governing non-linear partial differential equations are first transformed to a more convenient way before being solved numerically using the Keller-box method. The numerical values for the reduced Nusselt number and the reduced skin friction coefficient are obtained and illustrated graphically as well as temperature profiles and velocity profiles. Effects of the Prandtl number, Eckert number and nanoparticle volume fraction are analyzed and discussed. It is found that the Nusselt number for Al_2O_3-*Ag/Water* hybrid nanofluid is comparable with *Ag/Water* nanofluid with a reduction in skin friction coefficient. The preliminary results reports here are important as a reference in exploring the potential of hybrid nanofluid to reduce the production cost compared to the used of metal nanofluid.

Keywords: Free convection, hybrid nanofluid, circular cylinder, viscous dissipation

INTRODUCTION

Recent eras of technology saw the widely used of nanofluid as a cooling or heat transfer medium in many industrial, automotive and electrical devices. Nanofluid has a potential in the thermal management system such as liquid submerged cooling for transformer and electronic circuit board after the successful involvement in engine downsizing in automotive segment (Mohamed *et al.*, 2018). Better performance in thermal conductivity, viscosity, thermal diffusivity and convective heat transfer as well as no clogging are the reason for the employment of nanofluid compared to based fluid (Wong and De Leon, 2010).

It is known that the metal nanoparticles like copper *Cu* and silver *Ag* performed better in heat transfer capabilities compared to oxide nanoparticles, thanks to the nanoparticle's higher thermal conductivity. Unfortunately, this type of nanomaterial is expensive and not economical in mass production (Devi and Devi, 2017).

Present study investigates the flow and heat transfer on horizontal circular cylinder immersed in blended metal and oxide nanofluid called as hybrid nanofluid.

Considering the flow on a circular cylinder, there are many investigations have been done in the past decade, for example Salleh and Nazar (2010) and Sheikholeslami *et al.* (2012) who studied the Newtonian heating boundary conditions and magnetic effects on flow towards the horizontal circular cylinder. It is found that the skin friction coefficient is increasing at the middle of the cylinder before decreases to the end of the cylinder surface. Other researchers considered this topic with a Newtonian and non-Newtonian industrial fluid like power-law fluids by Chandra and Chhabra (2012), Bingham plastic fluid by Nirmalkar *et al.* (2014) and Bose *et al.* (2015), Casson fluid by Makanda *et al.* (2015) and nanofluid by Tham *et al.* (2012) and Mohamed *et al.* (2016). The nanofluid Buongiorno-Darcy model is employed and concluded that the increase in Brownian motion parameter and thermophoresis parameter has reduced the values of Nusselt number. Next, the flow and heat transfer immersed in a viscoelastic fluid, Jeffrey fluid, and viscoelastic nanofluid have been observed by Widodo *et al.* (2016), Zokri *et al.* (2017; 2018) and Mahat *et al.* (2018).

Recent studies on fluid flow on horizontal circular cylinder included the works from Gaffar *et al.* (2019), Yasin *et al.* (2020) and Alwawi *et al.* (2020) who investigate the heat transfer analysis of Casson nanofluid, ferrofluid, and third-grade fluid with magnetohydrodynamic effect. It is worth mentioning here that the ferrofluid is a nanofluid with ferrite nanoparticles. The ferrofluid heat transfer is dominance with the presence of a magnetic effect.

As for now, the experimental study regarding this topic is expensive and difficult to be realized. Some of the nanoparticles combinations in hybrid nanofluid are not yet able to being synthesizing, thus provided limited findings and knowledge. The approached from a numerical analysis based on a mathematical model is the alternative and relevant way to be considered. It is cheap, fast, and provided the theoretical knowledge for the hybrid nanofluid, therefore proposed an early idea about the fluid flow and heat transfer characteristics. Based on the literature studies, a study of free convection of hybrid nanofluid on a horizontal circular cylinder with the presence of viscous dissipation effect is never been done before, so the reported results in this study are new.

MATHEMATICAL FORMULATIONS

The horizontal circular cylinder with radius a, which is heated to a constant temperature T_w embedded in a hybrid nanofluid with ambient temperature T_∞ is considered. The physical model is shown in Fig 1. The orthogonal coordinates of $\bar{x}$ is measured along the cylinder surface, starting from the lower stagnation point $\bar{x}=0$, and $\bar{y}$ measures the distance normal from the surface. Under the assumptions that the boundary layer approximation is valid, the dimensional governing equations of steady free convection boundary layer flow are (Mohamed *et al.*, 2016; Devi and Devi, 2017) :

$$\frac{\partial \bar{u}}{\partial \bar{x}}+\frac{\partial \bar{v}}{\partial \bar{y}}=0, \tag{1}$$

$$\bar{u}\frac{\partial \bar{u}}{\partial \bar{x}}+\bar{v}\frac{\partial \bar{u}}{\partial \bar{y}}=\frac{\mu_{hnf}}{\rho_{hnf}}\frac{\partial^2 \bar{u}}{\partial \bar{y}^2}+\frac{(\rho\beta)_{hnf}}{\rho_{hnf}}g(T-T_\infty)\sin\frac{\bar{x}}{a}, \tag{2}$$

$$\bar{u}\frac{\partial T}{\partial \bar{x}}+\bar{v}\frac{\partial T}{\partial \bar{y}}=\frac{k_{hnf}}{(\rho C_p)_{hnf}}\frac{\partial^2 T}{\partial \bar{y}^2}+\frac{\mu_{hnf}}{(\rho C_p)_{hnf}}\left(\frac{\partial \bar{u}}{\partial \bar{y}}\right)^2, \tag{3}$$

subject to the boundary conditions

$$\begin{gathered}\bar{u}(\bar{x},0)=\bar{v}(\bar{x},0)=0,\ T(\bar{x},0)=T_w,\\ \bar{u}(\bar{x},\infty)\to 0,\ T(\bar{x},\infty)\to T_\infty,\end{gathered} \tag{5}$$

where $\bar{u}$ and $\bar{v}$ are the velocity components along the $\bar{x}$ and $\bar{y}$ axes, respectively. μ_{hnf} is the hybrid nanofluid dynamic viscosity, ρ_{hnf} is the hybrid nanofluid density, g is the gravity acceleration, β_{hnf} is the hybrid nanofluid thermal expansion, T is local temperature, $(\rho C_p)_{hnf}$ is the heat capacity of hybrid nanofluid, ν_{hnf} is the kinematic viscosity of hybrid nanofluid and k_{hnf} is the thermal conductivity of hybrid nanofluid which can be expressed as follows (Devi and Devi, 2017):

$$\begin{gathered}\nu_{hnf}=\frac{\mu_{hnf}}{\rho_{hnf}},\ \mu_{hnf}=\frac{\mu_f}{(1-\phi_1)^{2.5}(1-\phi_2)^{2.5}},\\ \rho_{hnf}=(1-\phi_2)\left[(1-\phi_1)\rho_f+\phi_1\rho_{s1}\right]+\phi_2\rho_{s2},\\ (\rho\beta)_{hnf}=(1-\phi_2)\left[(1-\phi_1)(\rho\beta)_f+\phi_1(\rho\beta)_{s1}\right]+\phi_2(\rho\beta)_{s2},\\ (\rho C_p)_{hnf}=(1-\phi_2)\left[(1-\phi_1)(\rho C_p)_f+\phi_1(\rho C_p)_{s1}\right]+\phi_2(\rho C_p)_{s2},\\ \frac{k_{hnf}}{k_{bf}}=\frac{k_{s2}+2k_{bf}-2\phi_2(k_{bf}-k_{s2})}{k_{s2}+2k_{bf}+\phi_2(k_{bf}-k_{s2})},\quad \frac{k_{bf}}{k_f}=\frac{k_{s1}+2k_f-2\phi_1(k_f-k_{s1})}{k_{s1}+2k_f+\phi_1(k_f-k_{s1})}.\end{gathered}$$

Note that the subscript $_{hnf}$, $_f$, $_{s1}$ and $_{s2}$ represent the physical properties of hybrid nanofluid, base fluid, alumina Al_2O_3, nanoparticle, and silver *Ag* nanoparticle, respectively.

In this study, initially 0.06 vol. solid nanoparticle of $Ag\ (\phi_2=0.06)$ is added into water based-fluid to form *Ag/Water* nanofluid. Next, 0.1 vol. solid nanoparticle of $Al_2O_3\ (\phi_1=0.1)$ is added into *Ag/Water* nanofluid to form the Al_2O_3-*Ag/Water* hybrid nanofluid namely. Next, it is introduced the governing non-dimensional variables:

$$\begin{gathered}x=\frac{\bar{x}}{a},\quad y=Gr^{1/4}\frac{\bar{y}}{a},\quad u=\frac{a}{\nu_f}Gr^{-1/2}\bar{u},\\ v=\frac{a}{\nu_f}Gr^{-1/4}\bar{v},\quad \theta(\eta)=\frac{T-T_\infty}{T_w-T_\infty},\end{gathered} \tag{6}$$

where θ are the rescaled dimensionless temperature of the fluid and $Gr=\dfrac{g\beta_f(T_w-T_\infty)a^3}{\nu_f^{\,2}}$ is a Grashof number. Using (6), (1)-(4) becomes

$$\frac{\partial u}{\partial x}+\frac{\partial v}{\partial y}=0, \tag{7}$$

$$u\frac{\partial u}{\partial x}+v\frac{\partial u}{\partial y}=\frac{\nu_{hnf}}{\nu_f}\frac{\partial^2 u}{\partial y^2}+\frac{(\rho\beta)_{hnf}}{\rho_{hnf}\beta_f}\theta\sin x, \tag{8}$$

$$u\frac{\partial \theta}{\partial x}+v\frac{\partial \theta}{\partial y}=\frac{k_{hnf}}{\nu_f(\rho C_p)_{hnf}}\frac{\partial^2\theta}{\partial y^2}+\frac{\nu_{hnf}}{\nu_f}\frac{\rho_{hnf}(C_p)_f}{(\rho C_p)_{hnf}}Ec\left(\frac{\partial u}{\partial y}\right)^2, \tag{9}$$

subject to the boundary conditions

$$\begin{gathered}u(x,0)=0,\ v(x,0)=0,\ \theta(x,0)=1,\\ u(x,\infty)\to 0,\ \theta(x,\infty)\to 0.\end{gathered} \tag{10}$$

Note that $Ec=\dfrac{\nu_f^{\,2}Gr}{a^2(C_p)_f(T_w-T_\infty)}$ is an Eckert number. In order to solve equations (7) to (9), the following functions are introduced:

$$\psi=xf(x,y),\quad \theta=\theta(x,y), \tag{11}$$

where ψ is the stream function defined as $u=\dfrac{\partial\psi}{\partial y}$ and $v=-\dfrac{\partial\psi}{\partial x}$ which identically satisfies Eq. (7). Substituting Eq. (11) into Eqs. (7)-(9), the following partial differential equations are obtained:

$$\begin{gathered}\frac{\nu_{hnf}}{\nu_f}\frac{\partial^3 f}{\partial y^3}+f\frac{\partial^2 f}{\partial y^2}-\left(\frac{\partial f}{\partial y}\right)^2+\frac{(\rho\beta)_{hnf}}{\rho_{hnf}\beta_f}\frac{\sin x}{x}\theta=\\ x\left(\frac{\partial f}{\partial y}\frac{\partial^2 f}{\partial x\partial y}-\frac{\partial f}{\partial x}\frac{\partial^2 f}{\partial y^2}\right),\end{gathered} \tag{12}$$

$$\begin{gathered}\frac{k_{hnf}(\rho C_p)_f}{k_f(\rho C_p)_{hnf}}\frac{1}{\Pr}\frac{\partial^2\theta}{\partial y^2}+f\frac{\partial\theta}{\partial y}=\\ x\left(\frac{\partial f}{\partial y}\frac{\partial\theta}{\partial x}-\frac{\partial f}{\partial x}\frac{\partial\theta}{\partial y}-xEc\frac{\nu_{hnf}}{\nu_f}\frac{\rho_{hnf}(C_p)_f}{(\rho C_p)_{hnf}}\left(\frac{\partial^2 f}{\partial y^2}\right)^2\right),\end{gathered} \tag{13}$$

where $\Pr=\dfrac{\nu_f(\rho C_p)_f}{k_f}$ is the Prandtl number. Other quantities are detailed as follows:

$$\frac{\nu_{hnf}}{\nu_f} = \frac{1}{(1-\phi_1)^{2.5}(1-\phi_2)^{2.5}\left[(1-\phi_2)+\left[(1-\phi_1)+\phi_1(\rho_{s1}/\rho_f)\right]+\phi_2(\rho_{s2}/\rho_f)\right]},$$
$$\frac{(\rho\beta)_{hnf}}{\rho_{hnf}\beta_f} = \frac{(1-\phi_2)\left[(1-\phi_1)\rho_f+\phi_1(\rho\beta)_{s1}/\beta_f\right]+\phi_2(\rho\beta)_{s2}/\beta_f}{(1-\phi_2)\left[(1-\phi_1)\rho_f+\phi_1\rho_{s1}\right]+\phi_2\rho_{s2}},$$
$$\frac{k_{hnf}(\rho C_p)_f}{k_f(\rho C_p)_{hnf}} = \frac{k_{hnf}/k_f}{(1-\phi_2)\left[(1-\phi_1)+\phi_1(\rho C_p)_{s1}/(\rho C_p)_f\right]+\phi_2(\rho C_p)_{s2}/(\rho C_p)_f},$$
$$\frac{\rho_{hnf}(C_p)_f}{(\rho C_p)_{hnf}} = \frac{(1-\phi_2)\left[(1-\phi_1)\rho_f+\phi_1\rho_{s1}\right]+\phi_2\rho_{s2}}{(1-\phi_2)\left[(1-\phi_1)\rho_f+\phi_1(\rho C_p)_{s1}/(C_p)_f\right]+\phi_2(\rho C_p)_{s2}/(C_p)_f}.$$

Next, the boundary conditions (10) become

$$f(x,0)=\frac{\partial f}{\partial y}(x,0)=0,\ \ \theta(x,0)=1,$$
$$\frac{\partial f}{\partial y}(x,\infty)\to 0,\ \ \theta(x,\infty)\to 0. \tag{14}$$

The physical quantities of interest are the skin friction coefficient C_f and the local Nusselt number Nu_x which given by

$$C_f=\frac{\tau_w}{\rho_f u_\infty^2},\qquad Nu_x=\frac{aq_w}{k_f(T_w-T_\infty)}. \tag{15}$$

The surface shear stress τ_w and the surface heat flux q_w are given by

$$\tau_w=\mu_{nf}\left(\frac{\partial \bar{u}}{\partial \bar{y}}\right)_{\bar{y}=0},\qquad q_w=-k_{nf}\left(\frac{\partial T}{\partial \bar{y}}\right)_{\bar{y}=0}. \tag{16}$$

Using variables in Eq. (6) and Eq. (11) give

$$C_f Gr^{1/4}=\frac{1}{(1-\varphi)^{2.5}}\left(x\frac{\partial^2 f}{\partial y^2}\right)_{\bar{y}=0}\ \text{and}$$
$$Nu_x Gr^{-1/4}=-\frac{k_{nf}}{k_f}\left(\frac{\partial\theta}{\partial y}\right)_{\bar{y}=0}. \tag{17}$$

Furthermore, the velocity profiles and temperature distributions can be obtained from the following relations:

$$u=f'(x,y),\qquad \theta=\theta(x,y). \tag{18}$$

NUMERICAL METHOD

The partial differential equations (12) and (13) subject to boundary conditions (14) are solved numerically using the Keller-box method. Keller-box method actually is an implicit finite difference method blend with Newton's method for linearization. Details regarding this method are clearly described by Na (1979), Cebeci and Cousteix (2005) and recently by Mohamed (2018). Keller-box method starts with reducing the equations to a first-order system. The finite difference method is taking part and linearized by using Newtons method. Then, the resulting algebraic equations are written in matrix-vector the form and lastly, being solved by the block tridiagonal elimination technique.

The algorithm of the Keller-box method is coded into MATLAB software to numerically compute. It is worth to noticed that the boundary layer thickness from 7 to 10 with step size $\Delta y=0.02$, $\Delta x=0.01$ are used in obtaining the converging and precise numerical results. The computation focused on the effects of a pertinent parameter which is the Prandtl number Pr, the Eckert number Ec and nanoparticle volume fraction for alumina $Al_2O_3\,(\phi_1)$ and silver $Ag(\phi_2)$. The values of thermophysical properties of water and nanoparticles consider are tabulated in Table 1. The calculation is obtained from the stagnation region $(x=0\,rad)$ until to the end of the cylinder surface $(x=\pi\,rad)$.

For comparison purposes, Tables 2 and 3 show the comparison values with previously published results. From both tables, it is found that the results agreed and in a good agreement, hence it is believed that whole results presents in this study are precise in computing numerically.

RESULTS AND DISCUSSION

The Figs. 1-8 are illustrated in order to get a clear view regarding the pertinent parameter effects on hybrid nanofluid flow and heat transfer. Figs. 2-5 show the variation of the reduced skin friction coefficient $C_f Gr^{1/4}$, reduced Nusselt number $Nu_x Gr^{-1/4}$, temperature profiles $\theta(y)$ and velocity profiles $f'(y)$ for various values of ϕ_1 and ϕ_2, respectively. From Fig. 1, it was found that values of the $C_f Gr^{1/4}$ is unique at the stagnation region $(x=0\,rad)$. At this point, the presents of nanoparticles gave no effects on friction. As flow passes through the cylinder body, the $C_f Gr^{1/4}$ increases when 0.06 vol. of silver *Ag* nanoparticles is added up into water-based fluid to form the *Ag/Water* $(\phi_1=0.0, \phi_2=0.06)$ nanofluid. The values of $C_f Gr^{1/4}$ then increase again with the adding 0.1 vol. of alumina Al_2O_3 nanoparticles into *Ag/Water* nanofluid to form the Al_2O_3-*Ag/Water* $(\phi_1=0.1, \phi_2=0.06)$ hybrid nanofluid. Further, the Al_2O_3-*Ag/Water* $(\phi_1=0.1, \phi_2=0.06)$ hybrid nanofluid is compare with *Ag/Water* $(\phi_1=0.0, \phi_2=0.16)$ nanofluid and it is found that the *Ag/Water* $(\phi_1=0.0, \phi_2=0.16)$ nanofluid have higher friction compared to Al_2O_3-*Ag/Water* $(\phi_1=0.1, \phi_2=0.06)$ hybrid nanofluid. Physically, the *Ag* has high density, hence score more friction in skin friction.

Fig. 2 shows the variation of the reduced Nusselt number $Nu_x Gr^{-1/4}$ for various values of ϕ_1 and ϕ_2. It was observed that the effects of changes in ϕ_1 and ϕ_2 are more significantly at the stagnation region. Further, it is noticed that the $Nu_x Gr^{-1/4}$ is decreasing along a cylinder surface. From Fig. 2, the Al_2O_3-*Ag/Water* $(\phi_1=0.1, \phi_2=0.06)$ hybrid nanofluid score highest values in $Nu_x Gr^{-1/4}$ compared to water-based fluid and *Ag/Water* $(\phi_1=0.0, \phi_2=0.06)$ nanofluid. These results are comparable with the high-cost *Ag/Water* $(\phi_1=0.0, \phi_2=0.16)$ nanofluid. It is clearly shown that the hybrid nanofluid which consists of the combination metal and low-cost oxide nanoparticles generate a comparable heat transfer capabilities with premium metal nanofluid.

Table 1. Thermophysical properties of water and nanoparticles.

Physical Properties	Water (f)	$Al_2O_3\,(\phi_1)$	$Ag(\phi_2)$	TiO_2	Cu
ρ (kg/m^3)	997	3970	10500	4250	8933
C_p (J/kg·K)	4179	765	235	686.2	385
k(W/m·K)	0.613	40	429	8.95	400

Table 2. Comparison values of $Nu_x Gr^{-1/4}$ with previous published results for various values of x when $\Pr = 1$ and $\phi_1 = \phi_2 = Ec = 0$.

x	Merkin (1976)	Nazar *et al.* (2002)	Molla et al. (2006)	Azim (2014)	Present
0	0.4214	0.4214	0.4214	0.4216	0.4213
$\pi/6$	0.4161	0.4161	0.4161	0.4163	0.4161
$\pi/3$	0.4007	0.4005	0.4005	0.4006	0.4007
$\pi/2$	0.3745	0.3741	0.3740	0.3742	0.3743
$2\pi/3$	0.3364	0.3355	0.3355	0.3356	0.3359
$5\pi/6$	0.2825	0.2811	0.2812	0.2811	0.2815
π	0.1945	0.1916	0.1917	0.1912	0.1934

Table 3. Comparison values of $C_f Gr^{1/4}$ with previous published results for various values of x when $\Pr = 1$ and $\phi_1 = \phi_2 = Ec = 0$.

x	Merkin (1976)	Nazar *et al.* (2002)	Molla et al. (2006)	Azim (2014)	Present
0	0.0000	0.0000	0.0000	0.0000	0.0000
$\pi/6$	0.4151	0.4148	0.4145	0.4139	0.4156
$\pi/3$	0.7558	0.7542	0.7539	0.7528	0.7534
$\pi/2$	0.9579	0.9545	0.9541	0.9526	0.9557
$2\pi/3$	0.9756	0.9698	0.9696	0.9678	0.9726
$5\pi/6$	0.7822	0.7740	0.7739	0.7718	0.7773
π	0.3391	0.3265	0.3264	0.3239	0.3356

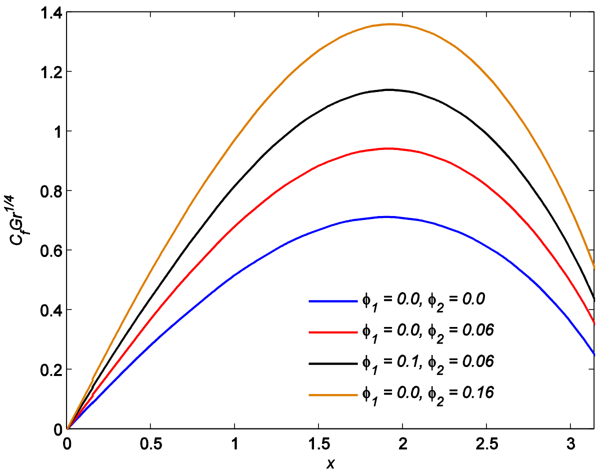

Fig. 1 Variation of $C_f Gr^{1/4}$ against x for various values of ϕ_1 and ϕ_2 when $\Pr = 7$ and $Ec = 0.1$

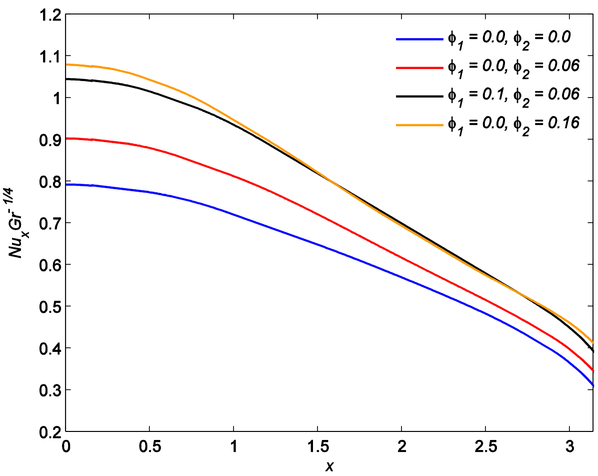

Fig. 2 Variation of $Nu_x Gr^{-1/4}$ against x for various values of ϕ_1 and ϕ_2 when $\Pr = 7$ and $Ec = 0.1$.

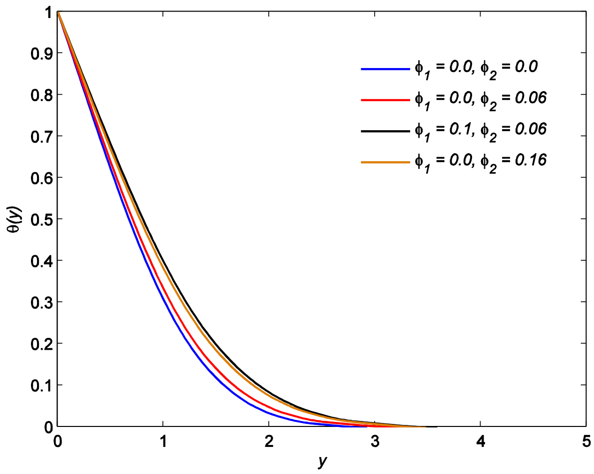

Fig. 3 Temperature profiles $\theta(y)$ against y for various values of ϕ_1 and ϕ_2 when $\Pr = 7$ and $Ec = 0.1$.

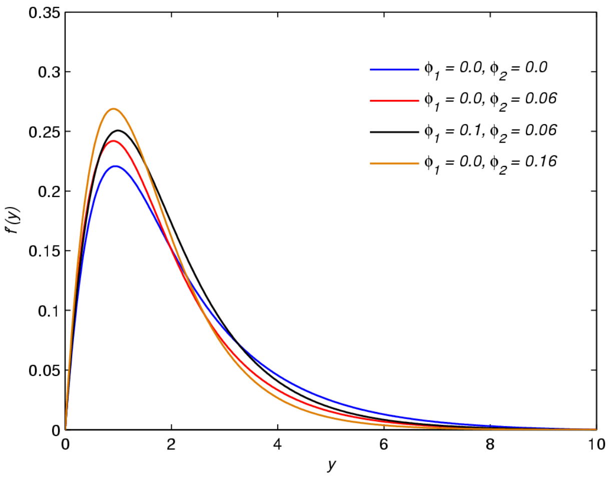

Fig. 4 Velocity profiles $f'(y)$ against y for various values of ϕ_1 and ϕ_2 when $\Pr = 7$ 7and $Ec = 0.1$.

The temperature profiles $\theta(y)$ and velocity profiles $f'(\eta)$ at a stagnation region $(x=0)$ for various values of ϕ_1 and ϕ_2 are illustrated in Figs. 3 and 4, respectively. It is shown the increase of nanoparticles has increased the thermal boundary layer thickness and the fluid velocity while reduced the velocity boundary layer thicknesses. The increase of nanoparticles in hybrid nanofluid has added up an extra thermal conductivity in fluid thus raised the thermal diffusivity and increase the thermal boundary layer thickness. In Figure 4, the presence of nanoparticles in fluid raised the fluid momentum which translates to the increasing in fluid velocity. This is realistic especially for nanofluid with denser nanoparticles like silver *Ag* in *Ag/Water* ($\phi_1 = 0.0, \phi_2 = 0.16$) nanofluid. The higher density nanofluid or hybrid nanofluid decelerate rapidly compare to water-based fluid due to friction between fluid and cylinder surface, thus lead to a reduction in velocity boundary layer thickness.

Next, Figs. 6 and 7 show the variation $C_f Gr^{1/4}$ and $Nu_x Gr^{-1/4}$ for various values of Pr and *Ec*, respectively. Both Figs. 4 and 5 agreed that the viscous dissipation effects *Ec* are negligible at stagnation region $(x=0)$. This is unsurprisingly and clearly stated in Eq. (13). The viscous dissipation effect is more pronounced in the middle of the cylinder body. It shows that the presence of viscous dissipation has promoted the skin friction effects as in Fig. 5 but reduced the convective heat transfer capability which represents by $Nu_x Gr^{-1/4}$ as shown in Fig. 6. Physically, the reduction in convective heat capabilities enhances the conductive heat transfer properties. Meanwhile, the increase of Pr results to the increase in $Nu_x Gr^{-1/4}$.

Lastly, the variations of $C_f Gr^{1/4}$ and $Nu_x Gr^{-1/4}$ for the various concentration of hybrid nanofluid are illustrated in Figs. 8 and 9, respecitively. The flow and heat transfer performance of *Al₂O₃-Ag/Water*$(\phi_1 = 0.1, \phi_2 = 0.06)$ hybrid nanofluid is compared with another hybrid nanofluid consist of titanium oxide TiO_2 and copper Cu nanoparticles. From both figures, it is learned that the different and appropriate combination nanoparticle in hybrid nanofluid provided desired flow and heat transfer characteristics (Devi and Devi, 2017). From Fig. 8, it is observed the values of $C_f Gr^{1/4}$ are not affected with the combination nanoparticles at the stagnation region $(x=0)$. It is more pronounced at the middle of the cylinder, different with $Nu_x Gr^{-1/4}$ which more significantly affected at the stagnation region as shown in Fig. 8. Further, it is noticed that the *Al₂O₃-Ag/Water* hybrid nanofluid score highest in $Nu_x Gr^{-1/4}$ followed by *Al₂O₃-Cu/Water* hybrid nanofluid. Specifically, *Ag* has the highest values of thermal conductivity compared *Cu, TiO₂* and *Al₂O₃*. Hence, any nanoparticle combination with *Ag* will provided high in heat transfer capability.

CONCLUSION

In this paper, the problem of free convection boundary layer flow over a horizontal circular cylinder in hybrid nanofluid was numerically studied. It was shown the effects of Prandtl number Pr, the Eckert number *Ec* and alumina *Al₂O₃*(ϕ_1) as well as silver *Ag*(ϕ_2) nanoparticles volume fraction for hybrid nanofluid.

As a conclusion, it is found that the increase of nanoparticles in nanofluid has increased the values of skin friction coefficient. The high-density nanoparticles like silver in nanofluid also contribute to a high in friction between fluid and cylinder surface. In industrial case, this situation damaging the component surface. From numerical investigation, the appropriate nanoparticles combination like alumina-silver in hybrid nanofluid may reduce these skin friction phenomena but yet still gave the heat transfer capabilities comparable to silver nanofluid. Noticed that alumina-silver hybrid nanofluid is cheaper to produce than silver nanofluid.

Next, it is observed that the Nusselt number shows a reducing variation along with the cylinder while skin friction experienced high in friction in the middle of the cylinder surface. The increase in Prandtl number results to the increase in Nusselt number while Eckert number which represented the viscous dissipation effects does contrary. Further, it is noticed that the high values of thermal conductivity nanoparticle like silver will provided high in heat transfer capability.

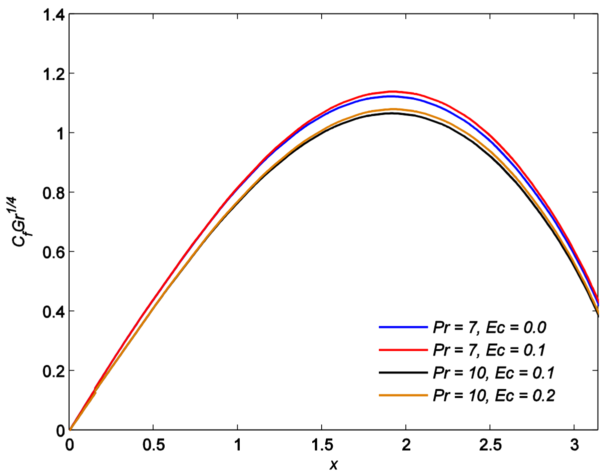

Fig. 5 Variation of $C_f Gr^{1/4}$ against x for various values of Pr and *Ec* when $\phi_1 = 0.1$ and $\phi_2 = 0.06$.

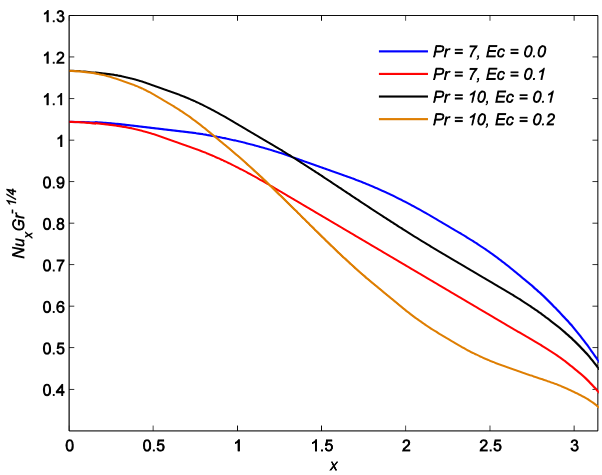

Fig. 6 Variation of $Nu_x Gr^{-1/4}$ against x for various values of Pr and *Ec* when $\phi_1 = 0.1$ and $\phi_2 = 0.06$.

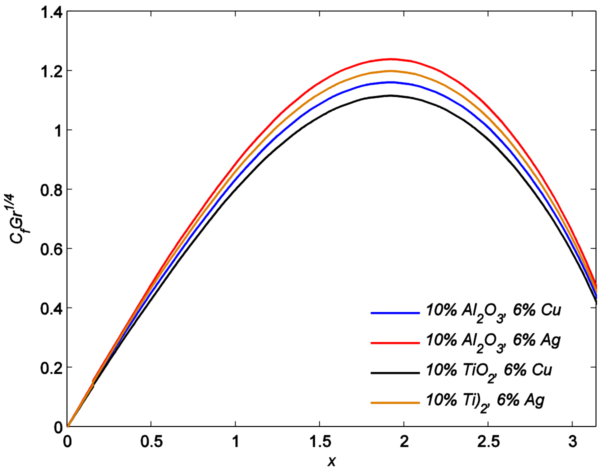

Fig. 7 Variation of $C_f Gr^{1/4}$ against x for various concentration of hybrid nanofuid when $\Pr = 7$ and $Ec = 0.1$.

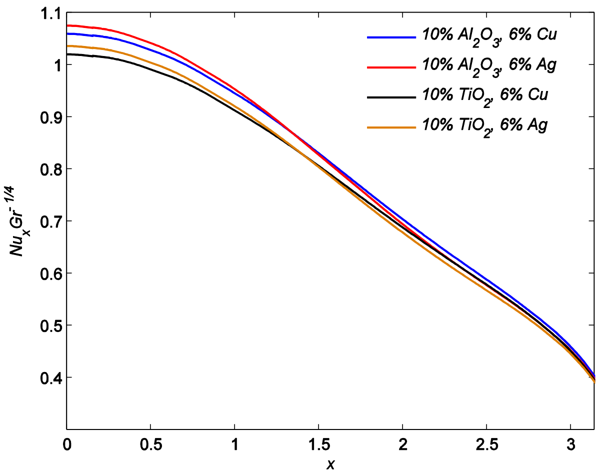

Fig. 8 Variation of $Nu_x Gr^{-1/4}$ against x for various concentration of hybrid nanofuid when $\Pr = 7$ and $Ec = 0.1$.

ACKNOWLEDGEMENT

Authors gratefully acknowledge the financial and facilities support from the Malaysia Ministry of Education (FRGS/1/2019/STG06/DHUAM/02/1), Universiti Malaysia Pahang and DRB-HICOM University of Automotive Malaysia.

REFERENCES

Alwawi, F. A., Alkasasbeh, H. T., Rashad, A. & Idris, R. 2020. Heat transfer analysis of ethylene glycol-based Casson nanofluid around a horizontal circular cylinder with MHD effect. *Proceedings of the Institution of Mechanical Engineers, Part C: Journal of Mechanical Engineering Science*, 0954406220908624.

Azim, N. H. M. A. 2014. Effects of viscous dissipation and heat generation on MHD conjugate free convection flow from an isothermal horizontal circular cylinder. *SOP Transactions on Applied Physics*, 1(3), 1-11.

Bose, A., Nirmalkar, N. & Chhabra, R. P. 2015. Effect of aiding-buoyancy on mixed-convection from a heated cylinder in Bingham plastic fluids. *Journal of Non-Newtonian Fluid Mechanics*, 220, 3-21.

Cebeci, T. & Cousteix, J. 2005. Modeling and computation of boundary layer flows. Springer.

Chandra, A. & Chhabra, R. P. 2012. Laminar free convection from a horizontal semi-circular cylinder to power-law fluids. *International Journal of Heat and Mass Transfer*, 55(11–12), 2934-2944.

Devi, S. S. U. & Devi, S. P. A. 2017. Heat transfer enhancement of Cu - Al2O3/water hybrid nanofluid flow over a stretching sheet. *Journal of the Nigerian Mathematical Society*, 36(2), 419-433.

Gaffar, S. A., Prasad, V. R., Reddy, P. R. & Khan, B. M. H. 2019. Radiative Flow of Third Grade Non-Newtonian Fluid From A Horizontal Circular Cylinder. 8(1), 673.

Mahat, R., Rawi, N. A., Kasim, A. R. M. & Shafie, S. 2018. Mixed convection flow of viscoelastic nanofluid past a horizontal circular cylinder with viscous dissipation. *Sains Malaysiana*, 47(7), 1617-1623.

Makanda, G., Shaw, S. & Sibanda, P. 2015. Effects of radiation on MHD free convection of a Casson fluid from a horizontal circular cylinder with partial slip in non-Darcy porous medium with viscous dissipation. *Boundary Value Problems*, 2015(1), 1-14.

Merkin, J. H. 1976. Free convection boundary layer on an isothermal horizontal cylinder. ASME/AIChe Heat Transfer Conference. St.Louis,USA.

Mohamed, M. K. A. 2018. Keller-box method: Partial differential equations in boundary layer flow of nanofluid. DRB-HICOM University Publisher, Pekan.

Mohamed, M. K. A., Noar, N. A. Z., Salleh, M. Z. & Ishak, A. 2016. Free convection boundary layer flow on a horizontal circular cylinder in a nanofluid with viscous dissipation. *Sains Malaysiana*, 45(2), 289-296.

Mohamed, M. K. A., Shah, N. M., Ismail, N. A., Jamil, F. C., Hashim, N., Salleh, M. Z. & Hashim, H. 2018. Convective boundary layer flow in a nanofluid. *Journal of Sciences and Management Research*, 3, 28-39.

Molla, M. M., Hossain, M. A. & Paul, M. C. 2006. Natural convection flow from an isothermal horizontal circular cylinder in presence of heat generation. *International Journal of Engineering Science*, 44(13–14), 949-958.

Na, T. Y. 1979. Computational methods in engineering boundary value problems. Academic Press, New York.

Nazar, R., Amin, N. & Pop, I. 2002. Free convection boundary layer on an isothermal horizontal circular cylinder in a micropolar fluid. *Proceedings of the 12th International Heat Transfer Conference*, Paris, Elsevier, 2, 525-530.

Nirmalkar, N., Bose, A. & Chhabra, R. P. 2014. Free convection from a heated circular cylinder in Bingham plastic fluids. *International Journal of Thermal Sciences*, 83, 33-44.

Salleh, M. Z. & Nazar, R. 2010. Free convection boundary layer flow over a horizontal circular cylinder with Newtonian heating. *Sains Malaysiana*, 39(4), 671-676.

Sheikholeslami, M., Gorji-Bandpay, M. & Ganji, D. D. 2012. Magnetic field effects on natural convection around a horizontal circular cylinder inside a square enclosure filled with nanofluid. *International Communications in Heat and Mass Transfer*, 39(7), 978-986.

Tham, L., Nazar, R. & Pop, I. 2012. Mixed convection boundary layer flow from a horizontal circular cylinder in a nanofluid. *International Journal of Numerical Methods for Heat & Fluid Flow*, 22(5), 576-606.

Widodo, B., Imron, C., Asiyah, N., Siswono, G. O. & Rahayuningsih, T. 2016. Viscoelastic fluid flow pass a porous circular cylinder when the magnetic field included. *Far East Journal of Mathematical Sciences*, 99(2), 173-186.

Wong, K. V. & De Leon, O. 2010. Applications of Nanofluids: Current and Future. *Advances in Mechanical Engineering*, 2010, 1-11.

Yasin, S., Mohamed, M., Ismail, Z. & Salleh, M. 2020. MHD free convection boundary layer flow near the lower stagnation point flow of a horizontal circular cylinder in ferrofluid. *MS&E*, 736(2), 022117.

Zokri, S. M., Arifin, N. S., Mohamed, M. K. A., Kasim, A. R. M., Mohammad, N. F. & Salleh, M. Z. 2018. Influence of viscous dissipation on the flow and heat transfer of a Jeffrey fluid towards horizontal circular cylinder with free convection: A numerical study. *Malaysian Journal of Fundamental and Applied Sciences*, 14(1), 40-47.

Zokri, S. M., Arifin, N. S., Mohamed, M. K. A., Salleh, M. Z., Kasim, A. R. M. & Mohammad, N. F. 2017. Mixed convection boundary layer flow over a horizontal circular cylinder in a Jeffrey fluid. *AIP Conference Proceedings*, 1842(1), 030007.